

"THE ROLE OF SPACE BORNE IMAGING RADARS IN ENVIRONMENTAL
MONITORING: SOME SHUTTLE IMAGING RADAR RESULTS IN ASIA"

M. L. Imhoff and C. H. Vermillion
NASA/Goddard Space Flight Center
Greenbelt, MD

(NASA-TM-101178) THE ROLE OF SPACE BORNE
IMAGING RADARS IN ENVIRONMENTAL MONITORING:
SOME SHUTTLE IMAGING RADAR RESULTS IN ASIA
(NASA) 23 p

N88-24844

CSCI 171

Unclas

G3/32 0147100

November 1986

The Role Of Space Borne Imaging Radars In Environmental Monitoring: Some Shuttle Imaging Radar Results In Asia

Marc L. Imhoff and C. H. Vermillion
NASA/Goddard Space Flight Center

ABSTRACT

The synoptic view afforded by orbiting Earth sensors can be extremely valuable for resource evaluation, environmental monitoring and development planning. For many regions of the world, however, cloud cover has prevented the acquisition of remotely sensed data during the most environmentally stressful periods of the year. This paper discusses how synthetic aperture imaging radar can be used to provide valuable data about the condition of the Earth's surface during periods of bad weather. Examples are given of applications using data from the Shuttle Imaging Radars (SIR) A & B for agricultural landuse and crop condition assessment, monsoon flood boundary and flood damage assessment, water resource monitoring and terrain modeling, coastal forest mapping and vegetation penetration, and coastal development monitoring. Recent SIR-B results in Bangladesh are emphasized, radar system basics are reviewed and future SAR systems are discussed.

INTRODUCTION

Remote sensing is a science of great interest and importance to both the developed and developing countries of the world. Since 1972 with the launch of the United States Earth Resources Satellite (Landsat) nations all over the world have been using the advantages of the synoptic view for monitoring the environment and surveying and assessing their natural resources. The Landsat instrument has been successfully used to map and inventory forests, make crop yield predictions, locate mineral deposits, facilitate land use planning, monitor water resources, and even make demographic maps. Presently, with the more advanced Landsat Thematic Mapper and SPOT sensors available, the uses for these instruments are becoming more numerous.

Despite the proven utility of passive multispectral instruments such as Landsat, SPOT, and AVHRR, there are many situations where the applicability of these sensors is severely limited. One major limitation is their inability to penetrate cloud cover. For many areas of the globe, the most environmentally stressful periods of the year are accompanied by a persistent veil of heavy wide-spread cloud cover. The acquisition of synoptic image data for these regions has historically been limited to chance i.e., those few cloud free days that coincide with a satellite overflight. The inability to acquire synoptic data during the high stress weather periods constitutes a very serious hiatus in data gathering which in turn limits the timeliness and effectiveness of resource surveys, environmental management programs, scientific investigations, and development activities. No where in the world is this hiatus more dramatic in its impact than in those regions experiencing the extreme

environmental changes brought on by a monsoon climate and its associated cycle of dehydration and flooding. The extremely complex ecological problems created by a monsoon climate, burgeoning population, and flood prone river systems are common to many developing nations and the lack of synoptic data during the wet season makes planning and development activities in these nations very difficult.

Radar remote sensing could literally provide a revolutionary thrust to planning activities and development programs in regions of the Earth that have monsoon or equatorial climates. The cloud penetrating capabilities of radar sensors permit the acquisition of clear images of the Earth surface showing the state of the surface hydrology, landuse, and agriculture during bad weather and/or the monsoon period. Radar could be used for making quick assessments of flooding and flood damage during the monsoon, rice agriculture yield estimates during the growing season, and water holding tank volume estimates throughout the year. Radar data showing surface hydrology during the monsoon period, could be used to model flow dynamics of flooding and run off and for planning future infrastructural development or flood control activities. These models could be further improved by using radar sensors to aid in the measurement of snow packs in mountain areas and model terrain for runoff predictions as a function of snowpack and/or precipitation.

Radar can also provide data that no other sensor can. In coastal areas, radar can be used to detect wave fronts and determine the direction of offshore currents. This information could be quite useful in measuring the effects of coastal development projects on coastal erosion. The radar also shows the actual structures which make up the coastal development and in coastal forest areas, radar may be a promising new tool for monitoring mangal or mangrove ecology.

This paper briefly describes some fundamental features of radar sensors, gives a short outline of past and future space borne SAR systems, and addresses some examples of how radar imagery has been used and is now being used in the Asian environment. A special emphasis will be made on the results of the Shuttle Imaging Radar (SIR) B project recently completed in the Peoples Republic of Bangladesh.

SPACE BORNE SYNTHETIC APERTURE RADAR SYSTEMS

Synthetic Aperture Radar (SAR) sensors, whether mounted on aircraft or on space platforms, basically follow the same set of design principals. Radar, being an active instrument does not require daylight to operate and the spatial resolution is not sensitive to changes in altitude. SAR sensors operate typically in the range of about 36 GHz or 0.83cm in wavelength which is the upper end of what is called K band to about 0.4 GHz or 77cm in wavelength which is the lower end of what is called the L-band [1]. The nominal L-band frequency and wavelength used for most satellite and aircraft SAR systems is around 1.3 GHz or 24 cm [2, 3, & 4]. The shorter wavelengths provide a higher resolution but are more sensitive to atmospheric effects and the longer wavelengths penetrate clouds cover, precipitation, very dry soils, and minor amounts of vegetation [2]. In addition to wavelength, a series of other system

parameters have a significant effect on the information content of the imagery. These parameters are polarization, incidence angle (look angle), antenna beam width, antenna gain, pulse repetition frequency (PRF), and the bits/sample if a digital system is used [5].

As far as targets or Earth surface features are concerned, the response that is measured and converted to a pixel with a brightness level is called backscatter and is usually measured in terms of Decibels. The intensity of the backscatter is dependent upon the physical characteristics of the target and its orientation to the radar and the dimensions of the target relative to the wavelength. The physical characteristics which create backscatter are often different from those that make a spectral response and as such may not be determined, except through inference, by Landsat or SPOT type sensors. The physical characteristics most prominent in determining radar response are: shape, texture, and dielectric constant [6]. In general large rough objects tend to appear as brighter pixels on an image while smoother targets appear as dark areas. Both the dielectric constant of the targets and their orientation to the radar, however, can completely alter the equation [5]. The point to be remembered is that radar sensors do not create images in accordance with our human sensory counterparts (our eyes), and that great care is required to match the SAR system parameters with the targets or landscape features of interest to achieve satisfactory results.

To date, there have been three SAR sensors mounted on orbiting space platforms: Seasat launched in 1978, SIR-A in 1981, and SIR-B in 1984. Their various physical characteristics can be seen in Table 1. Seasat's short lived program only permitted the acquisition of data for parts of North America, the Caribbean, and Western Europe [7] while SIRs-A & B acquired images globally [4 & 8]. SIR-B represented a significant step forward in SAR remote sensing as it was a digital system and could acquire data at different angles of incidence. The results obtained from the Seasat, SIR-A, and SIRB missions have been instrumental in demonstrating the utility of SAR sensors for resource evaluation and environmental monitoring.

The latter part of this decade and the 1990's will see several orbiting SAR systems. A future Shuttle mission SIR-C, the European ERS-1, and the Japanese JERS-1 will carry SAR sensors. Also plans are being made for a joint Canadian-American SAR satellite, Radarsat, and SAR systems will be carried on NASA's Space Station and Earth Observation System (Table 2). The SIR-C mission will be of very great scientific interest because of the great range of system options it will offer [8] while the ERS-1 and JERS-1 satellites will be of great value because of the extent of their temporal and areal coverage.

SAR APPLICATIONS IN THE ESCAP REGION

The applications of radar imagery are many and diverse. This is especially true if one includes aircraft mounted SAR remote sensing projects. A single paper can never present all the work that has been done by various investigators and scientists around the world. The following, therefore, is a short description of a few applications of space borne SAR imagery and is divided into a few general categories: Landuse and

Agriculture, Flood Damage Assessment and Water Resources, Terrain Analysis, and Forest and Coastal Resources and Coastal Development.

LANDUSE AND AGRICULTURE

If properly configured, SAR sensors can be valuable tools for mapping landuse and agriculture in the Asian environment. SAR data acquired during the wet season when rice paddies are full of water can be used to map villages, road networks, and the elevated levee system sectioning off the various paddy areas. Two very striking examples of this feature of SAR sensors can be noted in SIR-A data taken over villages and cultivated fields in Hebei-Shandong, China, and the Red River deltaic plain in Viet Nam [8]. In both cases the village and agricultural landuse patterns were dramatically more evident on the radar imagery than on their Landsat MSS counterparts (Figure 1). This effect is dramatic because of the physical dynamics of radar sensors and wet rice agricultural landuse. The close spatial proximity of flooded fields and raised levees, villages, canals, and road systems creates a great contrast in the radar images. The flooded rice fields tend to present a specular surface to the radar while the levees etc. act as reflectors. The occurrence of the two features side by side, as they are in wet rice agricultural areas, further creates a corner reflector effect which heightens the backscatter of the levees etc. thus increasing the contrast (Figure 2a).

Rice crops may be assessed using radar by observing how much the standing above-water-line biomass of the rice crop increases the backscatter on the normally dark flooded fields. This effect was noted in SIR-B imagery of an agricultural area in Southern Bangladesh which was taken at three angles of incidence (26, 46, and 58 deg.) on October 11, 12, and 13, 1984 (Table 3). In all three data sets the canal, transportation, and levee networks are clearly visible. After image filtering and enhancement it was found that even some of the individual dwellings could be delineated. Because this area is irrigated using tidal sluice gates and because of the storm activity during the last data take, the different water levels in the paddies could be noted in the images as a function of how much mature rice was exposed above the water line. When compared to aerial photography, it was found that the radar was showing how increased development in the area was deepening the water levels in the paddies as a result of the removal of soil in the paddies for creating raised earthworks. The subsequent absence of mature rice stalks in the deeper parts of each paddy was noted on the radar imagery as darker areas. The radar imagery clearly showed the effects of an increase in population on the productivity of the land (Figure 2b).

FLOOD DAMAGE ASSESSMENT AND WATER RESOURCES

The cloud penetrating capabilities of L-band SAR systems make them a natural choice for making immediate assessments of flooding and flood damage [10, 11, & 12]. The ability to acquire imagery at all times of the year regardless of cloud cover also makes SAR systems ideal for surveying water resources during the wet phase of the monsoon cycle.

In Bangladesh an effort was made to utilize data sets acquired by SIR-B and the Landsat 4 MSS to map flood boundaries and assess flood damage in an agricultural area on the Lower Meghna (Ganges) River near the town of Chandpur [13 & 14].

Although the wet phase of the monsoon was past, storm activity was still causing floods in the Mymensingh depression, Meghna, and Lower Meghna River areas. By chance a cloud free Landsat 4 MSS scene was acquired on September 27, 1984 which clearly showed the extent of the flood waters. Fifteen days later the Space Shuttle Challenger acquired SIR-B data over the same area. While the flood waters had mostly subsided, the SIRB data provided an excellent base map delineating the "normal" river levels and clearly outlining the local landuse patterns. A radar pass acquired a day later during heavy rainfall and severe winds showed hazardous areas in the river where severe currents and wave fronts were generated. Simple landcover categories and flood boundaries were defined on the Landsat data using spectral signature classification routines. Similar landuse categories were defined on the SIR-B data using a spatial smoothing filter and density slicing. The radar classification actually had a greater accuracy (85%) than the Landsat MSS (77%) due to a better separation of rice crop areas from villages and levees. Once categorized, the classification maps from the SIR-B and the Landsat data were digitally merged. From the merged data set it was possible to determine what landuse categories were flooded during September 27, 1984, the areal extent of flooding, and a table indicating the areal extent of each landuse class that was flooded (Figure 3, Table 4). From the merged multi-temporal multi-sensor data set, flood damage estimates could be made and flood dynamics observed. The areal estimates made using the merged Landsat and SIR-B imagery were also tied to river level measurements made near Chandpur. Using the combined radar, MSS, and river gauge data, a relationship could be made showing the number of hectares of land that will be flooded in the Chandpur area as a function of a rise in river level.

Radar imagery can be of great use in surveying water resources as well. In India, for example, radar could be used to help measure the holding capacities of water holding tanks or ponds and monitor their depletion. Radar images taken during the monsoon season could be used to establish maximum holding capacities of each pond and water use estimated as a function of the landuse surrounding each pond (Figure 4). These estimates could then be used to plan irrigation schemes for the next growing season.

TERRAIN ANALYSIS

One salient feature of SAR sensors is that they measure range. Every pixel on a radar image has an associated range measured as a distance (time) from the sensor to the ground. As a result, if images are acquired of the same area using different incidence angles or viewing points, stereo pairs can be made [15] (Figure 5) and the data exists to generate topographic data directly from the digital imagery [16] (Figure 6). From this data, elevation measurements can be computed and slope estimates can be made. This capability can have a significant future impact on terrain analysis for input to modeling in hydrology,

forestry, agriculture, geology, and landuse planning. Once refined, radar stereo mapping may be used to estimate snow packs in mountainous regions.

FOREST RESOURCES AND COASTAL RESOURCES AND DEVELOPMENT

Other areas of application where radar remote sensing has shown promise are forest resources and coastal resources and development. The application of SAR imagery for forest resources has historically met with varying success [17, 18, 19, 20, & 21]. One area of real demonstrated ability, however, is in the mapping of coastal forests or mangroves [9, 22, & 23]. SAR sensors at L-band wavelengths or longer have demonstrated an ability to penetrate vegetation canopies and delineate subcanopy soil areas where standing water is present [22, 24, 25, & 26]. This feature of L-band SAR imaging can be a useful tool for mapping the hydrodynamics of mangrove forests.

In Bangladesh, three SIR-B data sets were taken over the Sundarbans Forest Reserve near the Bay of Bengal. The data sets were examined for their ability to map forest stand characteristics and assessed for vegetation penetration [22]. The data sets were digitally preprocessed using carefully designed spatial filters to bring out image feature patterns that matched the spatial frequency of the desired forest information. As a result, definite image patterns emerged from the otherwise homogenous appearing data of the forest (Figure 7). On inspection, it was found that the image patterns did not closely match the forest classification maps, but that they clearly represented areas where water was standing within the forest. With further digital enhancement, color classes could be assigned to represent the relative tidal levels within the forest between the three data takes. The SIR-B imagery was in fact penetrating the 75% and greater, closed, 12.5 meter tall canopy and mapping the forest floor topography as a function of tidal flooding. This feature of radar remote sensing, which was also noted in Australia [23] and New Guinea [9], can be a useful tool for monitoring the mangrove ecology which depends upon a cycle of tidal and fresh water flooding. The ability to map relative island and coastal topography can also be useful for planning coastal development and reforestation activities.

SAR sensors can be valuable tools for coastal and marine applications as well. The first space borne SAR, Seasat, was designed for ocean observations and the SAR sensor to be carried by the ERS-1 is primarily designed for ocean applications as well. Although quite beyond the scope of this paper which deals mainly with land remote sensing, a few of the positive attributes of SAR sensors for coastal and marine applications should be mentioned. The surface structure of the ocean, in particular waves and wave fronts, create vivid and distinct features on radar imagery. The sensitivity of the radar to these features is a function of the system parameters of the SAR and the processing techniques used to create the imagery. Using SAR data and surface measurements, oceanographers have been able to deduce the ocean floor topography in some areas and determine the presence and direction of ocean currents. A great deal of success has been had in identifying currents and areas of turbulence near shore. This capability can be used to map and monitor

near shore currents and to model their potential effect on coastal erosion, shipping, and offshore mineral exploration. Radar can be very useful for monitoring the synergistic effects of coastal development projects such as harbor extensions or airport construction and offshore currents on coastal erosion. These findings can and have been applied to coastal development activities in Japan, Europe, and the United States [4].

A BRIEF NOTE ON RADAR IMAGE PROCESSING

In order to create an image from raw SAR data or the doppler history, a considerable amount of preprocessing is required, and, depending upon the type of end data product (digital or optical), and the intended application, some post processing or image enhancement techniques may be required as well. At both stages in the processing, a potential user may be asked to select certain options and these options will have a significant effect on the end product. Subsequently, processing options must be chosen intelligently with the intended use of the data in mind.

One of the more prominent preprocessing options that may be presented to the user for both optical and digital products is the number of "looks" used. Briefly stated, "looks" refers to a sampling process in the raw data which results in an averaging of data points. This sampling process is a technique used to diminish a phenomenon which occurs in radar data known as "speckle". While not really considered "noise" in an engineering sense, "speckle" causes a certain amount of visual distress to the viewer of SAR imagery and has historically made conventional interpretation of SAR images somewhat more difficult. "Look" processing smooths the image through the sampling and averaging process thus reducing the overt effects of speckle. However, this same process also degrades the spatial resolution of the end product, and since it requires more time to add "looks" to the processing a user may be charged accordingly. Care should be extended, therefore, to the selection of the number of looks one wants for producing an image.

A user may also be given the choice of getting optically or digitally processed imagery. If the SAR system data is processed optically, the user is generally presented with a black and white photographic record of the imagery. SAR data processed in this form cannot easily be manipulated or enhanced. Digital SAR data products, however, present the user with a wide range of post processing options that can substantially improve the utility of the data. Some very successful filtering, density slicing, and contrast enhancement techniques can be used to improve the applicability of the data for forestry, landuse mapping, coastal surveys, and general mapping [22, 27, and 28].

CONCLUSIONS

The potential applications of SAR data for resource assessment and environmental monitoring in the developed and developing world are numerous. The cloud penetrating capability of radar sensors makes them particularly useful for applications in those parts of the world having tropical or monsoon climates. For developing countries with monsoon climates where water resource management and flood control

activities are critical, the availability of SAR satellite data could literally revolutionize the planning and modeling processes.

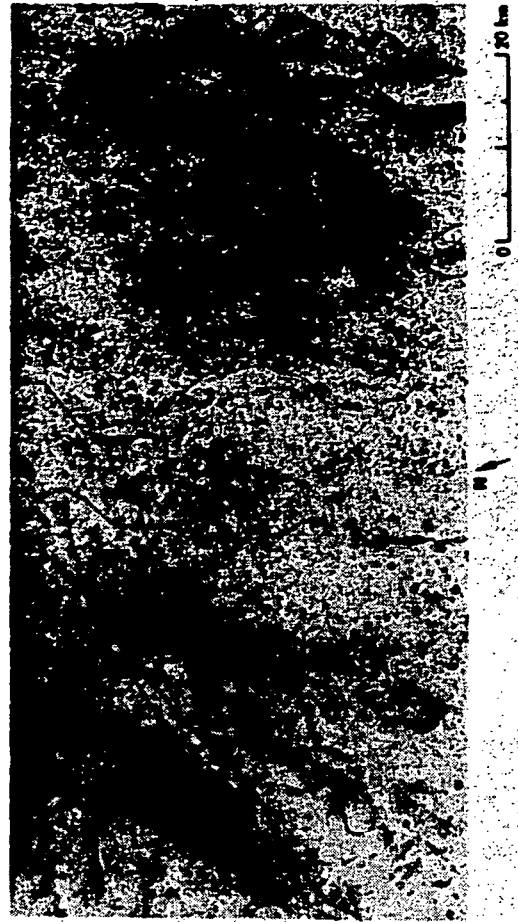
The availability of space borne radar data is rapidly becoming a reality. With the launches of the ERS-1 and JERS-1 satellites imminent, and the SIR missions continuing, there will be considerable SAR data available on a global basis by 1991.

What is needed now is the implementation of education programs and pilot projects so that a better understanding can be gained of the SAR system parameters required to meet the application needs of various nations. Because of its complex nature, SAR users of data must receive training. The many choices available for preprocessing the raw non-image radar data to create a base image, and the selection of post processing techniques to enhance and filter the imagery, are critical to its usefulness and interpretability. Without such knowledge and trained personnel, developing countries will miss the opportunity to guide the design of these future systems to fit their needs and be handicapped in their full use of the data. With this sort of training, however, the developing countries of the world will have gained a powerful new tool for managing their own development effectively and efficiently.

ACKNOWLEDGEMENTS

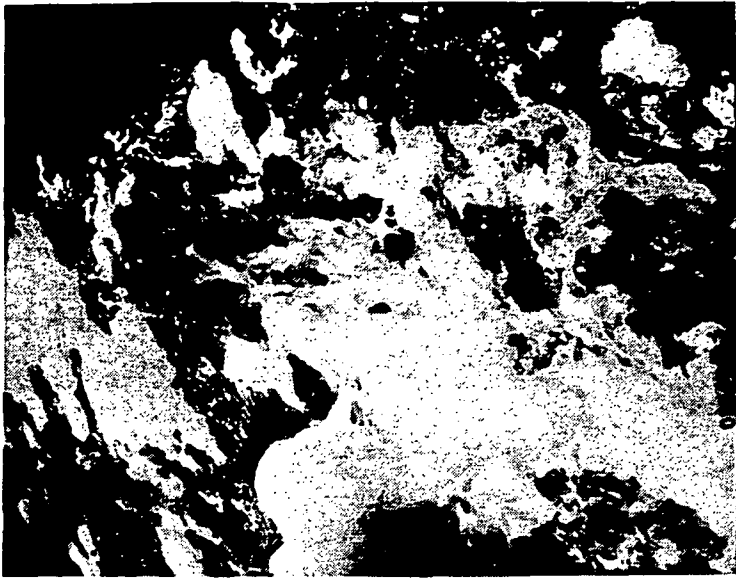
The authors would like to acknowledge the support of the Bangladesh Government and especially the Space Research and Remote Sensing Organization (SPARRSO), the Bangladesh Forestry Department, the Master Plan Organization, and Surface Water Hydrology II in the SIR-B project carried out in Bangladesh. Special thanks is extended to Drs. F. A. Khan and A. M. Choudhury of SPARRSO for their personal contributions.

The authors also appreciate the support of the British Overseas Development Administration in the Sundarbans forest survey project and the Jet Propulsion Laboratory of Pasadena, California for their work in all phases of the project.

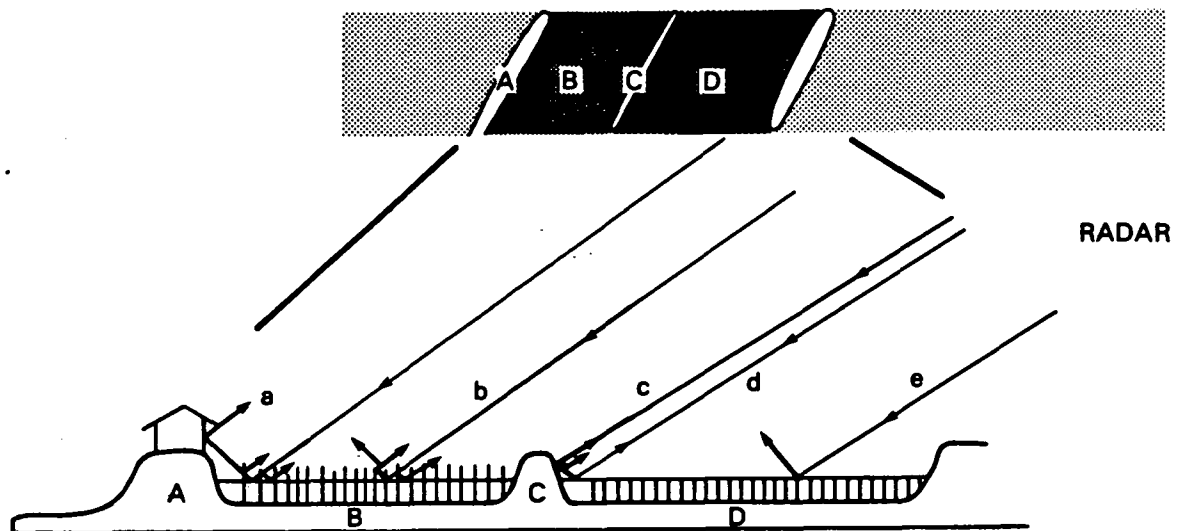


ORIGINAL PAGE IS
OF POOR QUALITY

FIGURE 1.



RADAR REFLECTANCE CHARACTERISTICS OF RICE AGRICULTURE — VILLAGE AREAS



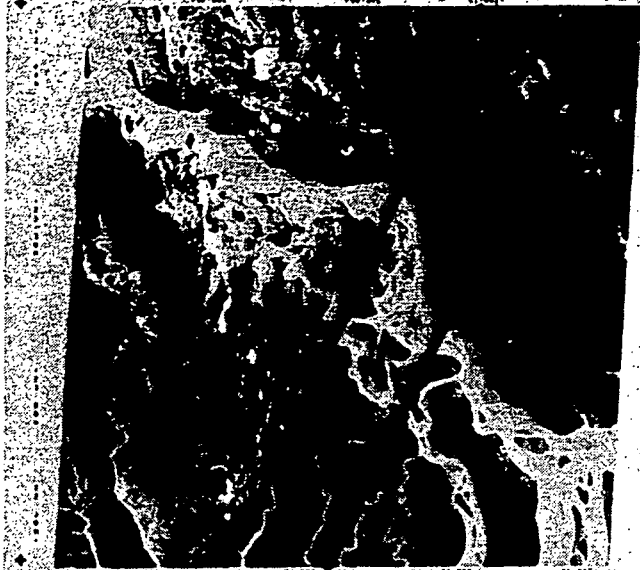
- A. Large embankment with dwelling
- B. Mature rice field standing crop
- C. Embankment
- D. Immature rice field little or no standing crop

- a. Specular component of rice radar interaction is returned to radar via dihedral corner reflector effect with nearby embankment.
- b. Mature rice causes dihedral corner reflections and increase in return to radar

- c. Direct reflection & dihedral corner reflection from embankments-dwellings and flooded fields
- d. Corner reflector effect high return
- e. Nearly a completely specular reflection (very low or no return to radar)

FIGURE 2.

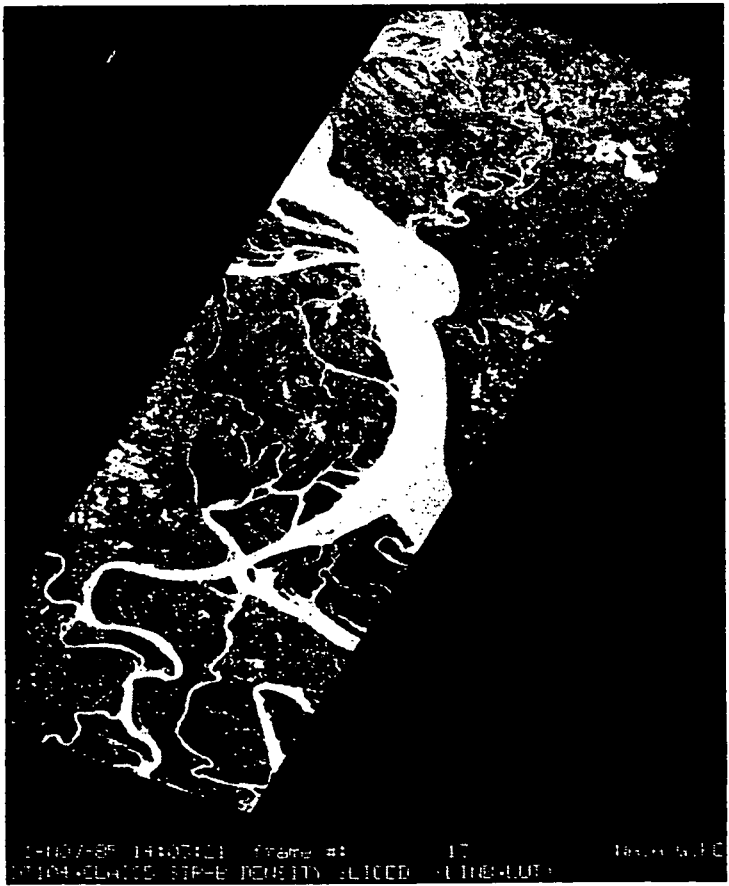
ORIGINAL PAGE IS
OF POOR QUALITY.



115 00000 23-064 00-22E 81
137 44 27000 400040343 C



115H-G3FC



1-10-85 14:07:01 frame #: 17 115H-G3FC
1104-ELWID-81P-8-DEWITY-ELICED-UTIS-LUT



115H-G3FC

FIGURE 3. ORIGINAL PAGE IS OF POOR QUALITY

ORIGINAL PAGE IS
OF POOR QUALITY

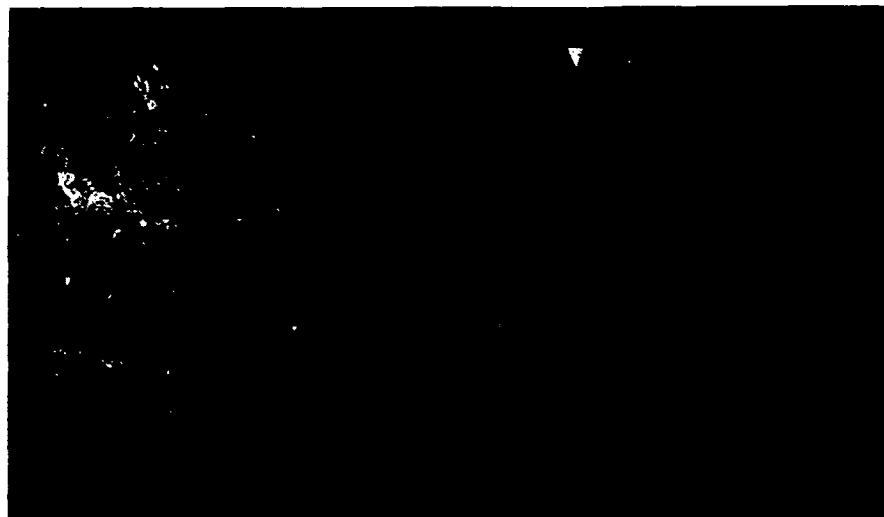


FIGURE 4.

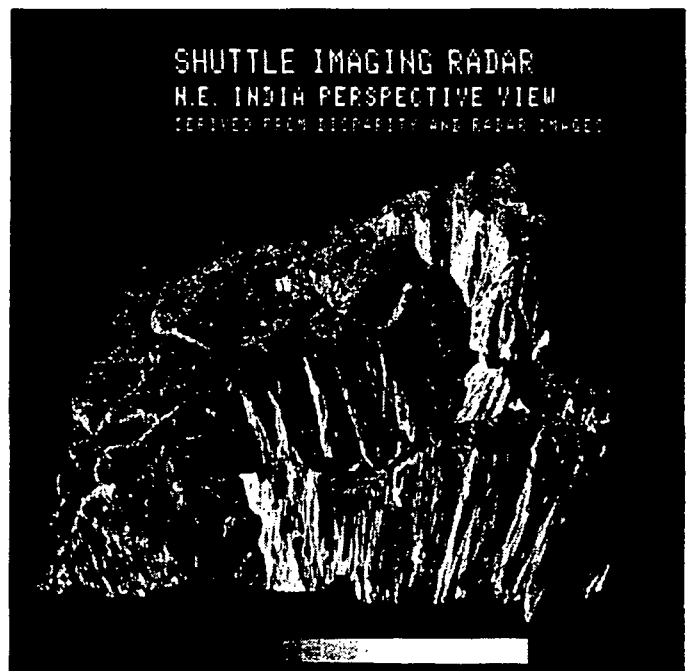
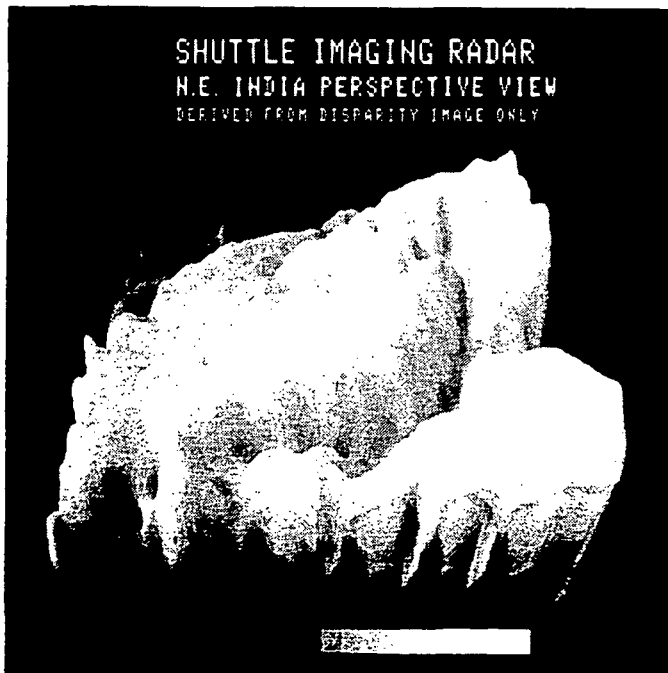
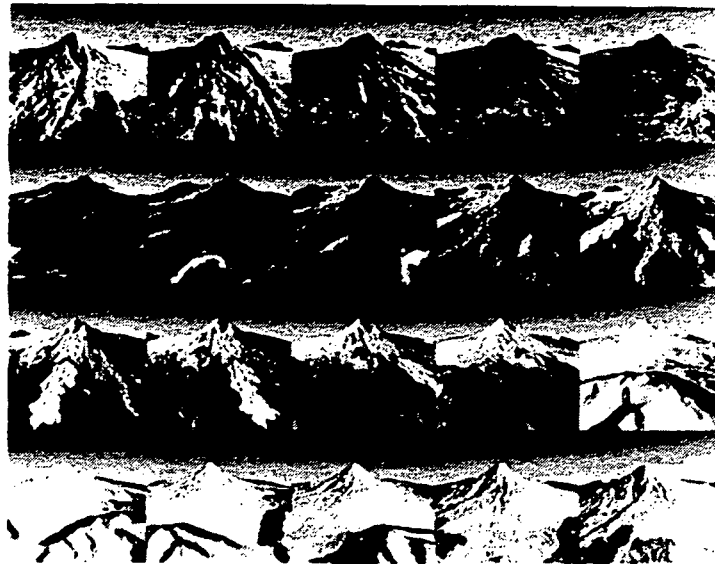
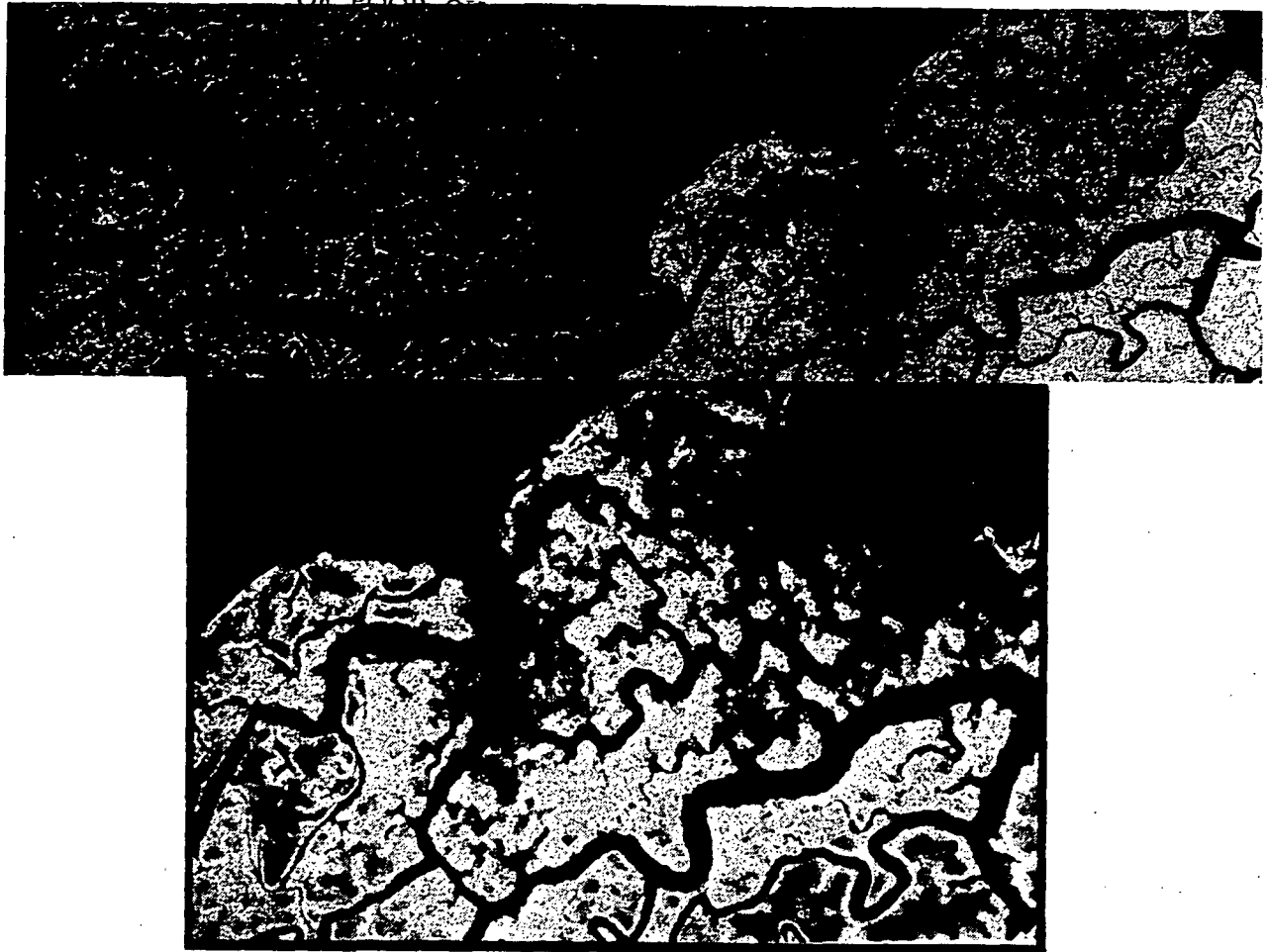


FIGURE 5.

ORIGINAL PAGE IS
OF POOR QUALITY

ORIGINAL PAGE IS
OF POOR QUALITY



TRANSECT PROFILE SHOWING TOPOGRAPHIC CONTOUR OF MANGROVE
FOREST AND ASSOCIATED RADAR PIXEL VALUES

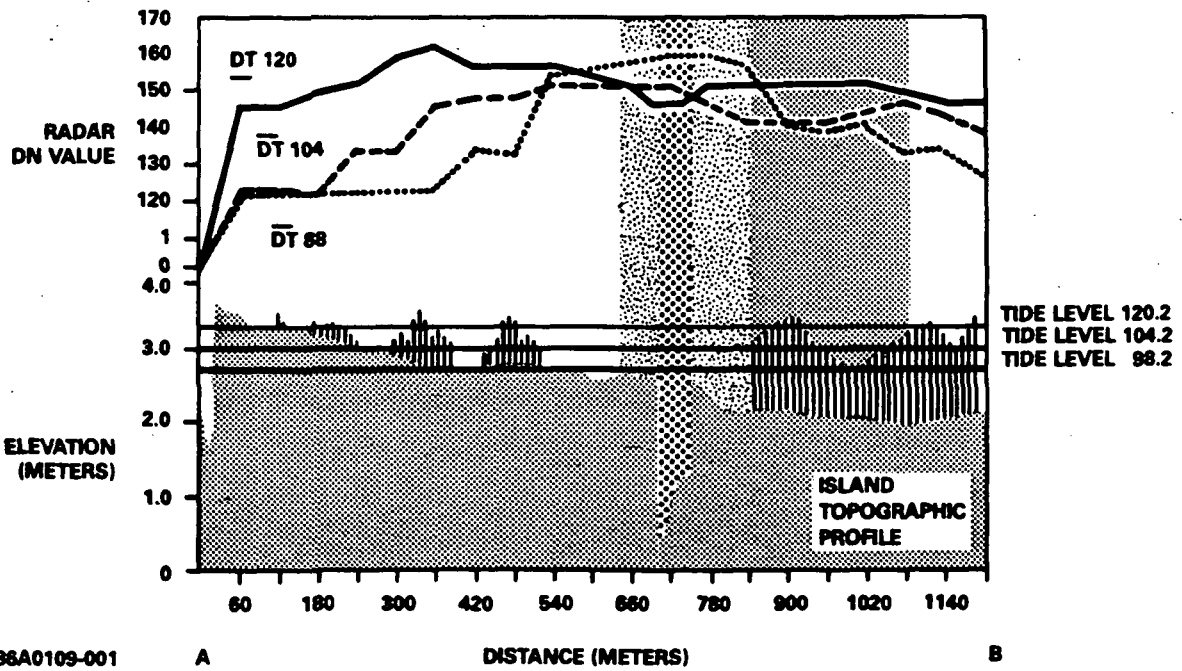


FIGURE 6.

ORIGINAL PAGE IS
OF POOR QUALITY

CAPTIONS FOR FIGURES

- FIGURE 1. (TOP) SIR-A image (left) and Landsat band 7 image (right) of Red River delta and floodplain in Northern Vietnam. (BOTTOM) SIR-A image (left) and Landsat band 7 image (right) of villages and agricultural fields in Hebei-Shandong, China. Both regions are important agricultural areas. The radar images clearly show the patterns of land use by delineating the rice paddy and village infrastructure. The Landsat images, in both cases, show less structural detail.
- FIGURE 2. (TOP LEFT) Limb photograph of Bay of Bengal and Southern Bangladesh. Taken from the Shuttle Challenger during the SIR-B mission. Most of the land surface is hidden by cloud cover. (BOTTOM) Diagram showing how the juxtaposition of flooded fields and raised earthworks create strong contrast in wet rice and jute agricultural fields. The taller and denser the standing crop the brighter the radar response in the paddies and the lesser the overall image contrast. (TOP RIGHT) Merged multiple-incidence angle SIR-B data set of agricultural area near the Bola River in Southern Bangladesh. The merged image consists of Data Take 88 (58 deg.) -Green, Data Take 104 (46 deg.) Blue, and Data Take 120 (26 deg.) -Red. The extremely bright areas denote raised earthworks or roads, levees, canals, and homesteads. The dark areas represent the flooded rice fields with the darkest part of the fields being relatively devoid of a standing crop. Brighter areas in fields near earthworks represent taller standing crops. All three data takes making this composite were acquired through heavy cloud cover.
- FIGURE 3. (TOP LEFT) Landsat MSS Scene of Chandpur survey area in Southern Bangladesh. SIR-B track is outlined on the scene. (TOP RIGHT) Landsat MSS landcover classification of Chandpur survey area on the Lower Meghna (Ganges) river in Southern Bangladesh. Classification shows Agriculture and Village areas, Flooded Land, and Surface water. (TOP RIGHT) Spatially filtered and density sliced SIR-B image of Chandpur survey area. Density slices were classified as Villages/Infrastructure, Agricultural Land, Surface Water, and Scrub Vegetation. (BOTTOM LEFT) SIR-B landcover map overlaid on Landsat landcover classification map (center strip in image). The digital merger of the two data sets permitted an assessment of temporal change, damage caused by flooding, and the modeling of areal inundation as a function of rise in river gauge level (see Table 4).
- FIGURE 4. SIR-A images of Western India near the Thar Desert. Images shows water tanks or ponds (dark spots) and surrounding village and agricultural development (bright areas). Such data acquired during the peak wet season could be used to establish maximum holding capacities for ponds (tanks) and reservoirs. India-Pakistan border area is shown in center of bottom image.

FIGURE 5. (TOP) Composite views of Mount Shasta in Northern California created by merging an enhanced radar image with an elevation model created from two radar data sets collected during the SIR-B at 30 degrees and 64 degrees. (Caption adapted from the work of Dr. Franz Leberl of the Vexcel Corporation, and Dr. Mike Kobrick of (JPL). (BOTTOM) Stereo image created from SIR-B data of the Shillong Plateau area in Eastern India. This single view was created by merging a radar image with an elevation model created directly from two incidence angles (26 and 46 degrees) using the Massively Parallel Processor located at NASA/Goddard Space Flight Center. This image is only one of an infinite number of possible views. Terrain parameters such as slope angles and slope area can be computed from the data and input to runoff models. (Caption courtesy of Drs. H.K. Ramapriyan and J. Strong NASA/ Goddard Space Flight Center).

FIGURE 6. (TOP) One of three SIR-B data takes over the Sundarbans Forest Reserve and agricultural areas in Southern Bangladesh. The SIR-B data were acquired at night through heavy cloud cover. The mangrove forests are shown as the relatively homogenous bright area at the image left. The agricultural fields are located in the right part of the image. This image was taken at an incidence angle of 46 degrees and represents a basic 4 look unenhanced digital product. (CENTER) A digitally enhanced SIR-B image data product created from the standard image shown above. Median filters matched to the spatial frequency of natural forest and terrain features were used to extract distinct image patterns from the otherwise homogenous appearing data set. The brighter areas on the image represent areas where standing water is present beneath the 12.5 meter tall 75% to 100% closed tree canopy. A topographic map of the forest floor could be inferred by comparing SIR-B imagery acquired at different times as a function of tidal inundation. (BOTTOM) Survey transect showing topographic contour through one of the islands in the Sundarbans Forest. Tide levels for each data take and digital numbers for each radar data set along the transect are shown.

TABLE 1 System Specifications for Seasat, SIR-A and SIR-B
Synthetic Aperture Radars

| <u>Parameters</u> | <u>Seasat</u> | <u>SIR-A</u> | <u>SIR-B</u> |
|---------------------|----------------|---------------|---------------|
| Orbital altitude | 800km | 260 km | 225 km |
| Orbital inclination | 108 deg | 38 deg | 57 deg |
| Frequency | 1.28 GHz | 1.28 GHz | 1.28 GHz |
| Polarization | HH | HH | HH |
| Look angle(s) | 23 deg | 47 deg | 15-60 deg |
| Swath width | 100 km | 50 km | 20-50 km |
| Peak power | 1 kW | 1 kW | 1 kW |
| Antenna dimensions | 10.74 x 2.16 m | 9.4 x 2.16 | 10.7 x 2.16 |
| Antenna gain | | 33.6 dB | 33.0 dB |
| Bandwidth | 19 MHz | 6 MHz | 12 MHz |
| Azimuth resolution | 25 m | 40 m (6 look) | 25 m (4 look) |
| Range resolution | 25 m | 40 m | 58-17 m |

TABLE 2 Future Space Borne SAR Systems

| <u>System</u> | <u>Origin</u> | <u>Band</u> | <u>Polarization</u> | <u>Incidence Angle</u> | <u>Approximate Date of Launch</u> |
|---------------------|-----------------------|-------------|------------------------------|------------------------|-----------------------------------|
| ERS-1 | European Space Agency | C | VV | 25° | 1989 |
| SIR-C | United States | X,C,L | HH, VV, VH, HV, (L&C), WV(X) | 15°-60° | 1990 |
| JERS-1 | Japan | L | HH | 42° | 1991 |
| EOS (SIR-E) | United States | L,C,X | HH,VV,HV, (L&C), WV(X) | 15°-60° | 1993 |
| EOS (GLORI & HIRIS) | United States | C, VIS/IR | VV | -- | -- |

TABLE 3 SIR-B Radar Acquisitions Over Bangladesh

| <u>Data Take #</u> <u>DT</u> | <u>Date Acquired</u> <u>(GMT)</u> | <u>Incidence Angle</u> | <u>Bit/Sample</u> | <u>S/N</u> | <u>Resolution Range</u> | <u>Ground (M) Azimuth</u> |
|---------------------------------|--------------------------------------|------------------------|-------------------|------------|-------------------------|---------------------------|
| 88 | Oct. 10, 1984 | 57.8° | 5 | 3.73 | 16.6 | 31.1 |
| 104 | Oct. 11, 1984 | 45.6° | 5 | 6.49 | 19.8 | 33.7 |
| 120 | Oct. 12, 1984 | 25.8° | 4 | 5.83 | 32.3 | 28.3 |

TABLE 4 Flood Area Inundation Summary (Hectares)

| SIR-B (Oct. 12, 1984) | /LANDSAT MSS (Sept. 27, 1984) | | |
|--------------------------|-------------------------------|------------------------------|-------------------------|
| | Water (non-turbid) | Flood Water (very turbid) | Agriculture/ Village |
| Water (non-flood) | 42,062 | 6,098 | 7,550 |
| Agriculture | *25,483 | *33,069 | 75,624 |
| Village | * 520 | * 1,948 | 11,439 |
| Scrub Vegetation | * 381 | * 1,638 | 494 |
| | | Total area | 206,306 |

* The sum of these components were used to estimate number of hectares of land flooded by river overflow on Sept. 27, 1984.

A total of 63,039 hectares in the survey area (206,306 ha. total) were considered flooded on Sept. 27, 1984. Of that, approximately 58,552 hectares were estimated to be agricultural land, 2,468 hectares were homesteads or other infrastructure and 2,019 hectares were scrub lands at the river margins.

REFERENCES

- [1] Lindenlaub, John C., 1976. "Side Looking Airborne Radar", Fundamentals of Remote Sensing Minicourse, Purdue University, West Lafayette, Indiana, USA.
- [2] Cimino, J. B. and C. Elachi, 1982. Shuttle Imaging Radar-A (SIR-A) Experiment, NASA/JPL Publication 82-77, National Aeronautics and Space Administration, Washington D.C.
- [3] Thompson, T. W., 1983. A User's Manual for the NASA/JPL Synthetic Aperture Radar and the NASA/JPL L- and C-band Scatterometers, NASA/JPL Publication 83-38, Pasadena, California.
- [4] Ford, J. P., J. B. Cimino, B. Holt, and M. R. Ruzek, 1986. Shuttle Imaging Radar Views the Earth From Challenger: The SIR-B Experiment, NASA/JPL Publication 86-10, Pasadena, California.
- [5] NASA/JPL, 1982. The SIR-B Science Plan, NASA/JPL Publication 82-78, Pasadena, California.
- [6] Hoffer, R. M., 1976. Interpretation of Radar Imagery, Fundamentals of Remote Sensing Minicourse, Purdue University, West Lafayette, Indiana.
- [7] Ford, J. P., R. G. Bloom, M. L. Bryan, M. I. Daily, T. H. Dixon, C. Elachi, and E. C. Xenos, 1980. Seasat Views North America, the Caribbean, and Western Europe With Imaging Radar, NASA/JPL Publication 80-67, Pasadena, California.
- [8] Ford, J. P., J. B. Cimino, C. Elachi, 1983. Space Shuttle Columbia Views the World With Imaging Radar: the SIR-A Experiment, NASA/JPL Publication 82-95, Pasadena, California.
- [9] NASA/JPL, 1983. Shuttle Imaging Radar-C (SIR-C) Executive Summary, NASA/JPL Publication 83-47, Pasadena, California.
- [10] Lowry, R.T., N. Mudry, and E. J. Langham, 1979. "A Preliminary Analysis of SAR Mapping of the Manitoba Flood, May 1979", Satellite Hydrology; Proceedings of the Fifth Annual William T. Pecora Memorial Symposium on Remote Sensing, Sioux Falls, South Dakota.
- [11] Ormsby, J. P., J. P. Blanchard, and A. J. Blanchard, 1985. "Detection of Lowland Flooding Using Microwave Systems", American Soc. of Photogrammetry, Vol. LI, No. 3, pp. 317-328.
- [12] Krohn, M. D., N. M. Milton, and D. B. Segal, 1983. "Seasat Synthetic Aperture Radar (SAR) Response to Lowland Vegetation Types in Eastern Maryland and Virginia". Journal of Geophysical Research, Vol. 88, No. c3, pp. 1937-1952.
- [13] Imhoff, M. L., C. H. Vermillion, M. Story, and F. Polcyn, 1986. "Space-Borne Radar for Monsoon and Storm Induced Flood Control

Planning in Bangladesh: A Result of the Shuttle Imaging Radar-B Program". Man's Role In Changing the Global Ecology Conference, Venice, Italy, Science of the Total Environment, Elsevier Science Publishers, Amsterdam, the Netherlands.

- [14] Imhoff, M. L., C. Vermillion, M. H. Story, A. M. Chaudhury, A. Gafoor, and F. Polcyn, 1986. "Monsoon Flood Boundary Delineation and Damage Assessment Using Space Borne Imaging Radar and Landsat Data". Accepted for publication in Photogrammetric Engineering and Remote Sensing.
- [15] Leberl, F., G. Domik, J. Raggam, and M. Kobrick, 1986. "Radar Stereomapping Techniques and Application to SIR-B Images of Mount Shasta". IEEE Transactions on Geoscience and Remote Sensing, Vol. GE-24, No. 4, pp. 473-481.
- [16] Ramapriyan, H. K., J. P. Strong, Y. Hung, and C. W. Murray Jr., 1986. "Automated Matching of Pairs of SIR-B Images For Elevation Mapping". IEEE Transactions on Geoscience and Remote Sensing, Vol. GE-24, No. 4, pp. 462-471.
- [17] Smit, G. Sicco, 1975, "Will the Road to Green Hell Be Paved With SIAR (A Case Study of Tropical Rain Forest Type Mapping in Colombia)", ITC Journal 1975, Vol. 2.
- [18] Trevett, S. W., 1978. "Vegetation Mapping of Nigeria From Radar", 12th International Symposium on Remote Sensing of Environment, April 20-26, 1978 Manila, Philippines Proceedings, Vol.3, ERIM, Ann Arbor Michigan.
- [19] Gelrett, R. H., L. F. Dellwig, and J. E. Base, 1978. "Increased Visibility From the Invisible, A Comparison of Radar and Landsat in Tropical Environments, 12th International Symposium on Remote Sensing of Environment, April 20-26, 1978, Manila, Philippines Proceeding, Vol. 3, ERIM, Ann Arbor, Michigan.
- [20] Cimino, J. B., A. Brandani, D. Casey, J. Rabassa, and S. D. Wall, 1986. "Multiple Incidence Angle SIR-B Experiment Over Argentina: Mapping of Forest Units", IEEE Transactions on Geoscience and Remote Sensing, Vol. GE-24, No. 4, pp. 498-509.
- [21] Hoffer, R., D. F. Lozano-Garcia, D. D. Gillespie, P. W. Mueller, and M. J. Ruzek, 1986. "Analysis of Multiple Incidence Angle SIR-B Data for Determining Forest Stand Characteristics", 2nd Space Borne Imaging Radar Symposium, May 1986, JPL, Pasadena, California.
- [22] Imhoff, M., M. Story, C. Vermillion, F. Khan, and F. Polcyn, 1986. "Forest Canopy Characterization and Vegetation Penetration Assessment With Space-Borne Radar". IEEE Transactions on Geoscience and Remote Sensing, Vol. GE-24, No. 4, pp. 535-542.

- [23] Milne, T., 1986. "SIR-B Results in Australia", 2nd Space Borne Imaging Radar Symposium, May 1986, JPL, Pasadena, California.
- [24] Waite, W. P., and H. C. MacDonald, 1971. "Vegetation Penetration with K-band Imaging Radars", IEEE Transactions on Geoscience and Electronics, Vol. GE-9, No. 3, pp. 147-155.
- [25] MacDonald, H. C., W. P. Waite, and J. S. Demarke, 1980. "Use of Seasat Satellite Radar Imagery for the Detection of Standing Water Beneath Forest Vegetation". American Society of Photogrammetry Technical Meeting, Niagra Falls, N.Y., pp. RS-3-B-1 to RS-3-B-13.
- [26] Waite, W. P., H. C. MacDonald, V. H. Kaupp, and J. S. Demarke, 1981. "Wetland Mapping With Imaging Radar", 1981 International Geoscience and Remote Sensing Symposium, IEEE June 8-10, Washington D.C.
- [27] Daily, M., 1983. "Hue-Saturation-Intensity Split-Spectrum Processing of Seasat Radar Imagery". Photogrammetric Engineering and Remote Sensing, Vol.49, No. 3, pp. 349-355.
- [28] Lee, Jong-Sen, 1981. "Speckle Analysis and Smoothing of Synthetic Aperture Radar Images". Computer Graphics and Image Processing, Vol. 17, pp. 24-32.
- Lee, Jong-Sen, 1983. "Digital Image Smoothing and the Sigma Filter". Computer Vision Graphics and Image Processing, Vol. 24, pp. 255-269.